ACS APPLIED MATERIALS & INTERFACES

Research Article

www.acsami.org

Heparin Loading and Pre-endothelialization in Enhancing the Patency Rate of Electrospun Small-Diameter Vascular Grafts in a Canine Model

Chen Huang,[†,‡,§] Sheng Wang,*[,†,⊥] Lijun Qiu,[‡] Qinfei Ke,[§] Wei Zhai,[⊥] and Xiumei Mo*[,‡]

[‡]State Key Laboratory for Modification of Chemical Fibers and Polymer Materials and [§]College of Textiles, Donghua University, Shanghai 201620, China

[⊥]Department of Critical Care Medicine, Shanghai Tenth People's Hospital, Tongji University, Shanghai 200072, China

Supporting Information

ABSTRACT: We herein proved that the two commonly used antithrombotic methods, heparin loading and pre-endothelialization could both greatly enhance the patency rate of a small-diameter graft in a canine model. Tubular grafts having an inner diameter of 4 mm were prepared by electrospinning poly(L-lactide-co-ε-caprolactone) (P(LLA-CL)) and heparin through a coaxial electrospinning technique. Seventy-two percent of heparin was found to be released sustainably from the graft within 14 days. To prepare the pre-endothelialized grafts, we seeded endothelial cells isolated from the femoral artery and cultured then dynamically on the lumen until a cell monolayer was formed. Digital subtraction angiography (DSA) and color Doppler flow imaging (CDFI) were used to monitor the patency without sacrificing the animals. Histological analyses revealed that following the direction of blood flow, a cell monolayer was formed at the proximal end of the heparin-loaded grafts, but such a monolayer could be found in the middle or distal region of the grafts. In contrast, the whole luminal surface of the pre-endothelialized graft was covered by a cell monolayer, suggesting the in vivo survival of the preseeded cells. This demonstrated that heparin was a comparatively simple method to achieve good patency, but the pre-endothelialization had better mechanical properties and cellular compatibility.

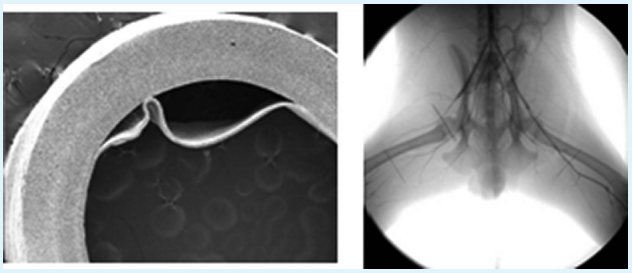

KEYWORDS: *heparin, endothelialization, electrospun, vascular grafts, patency rate, canine*

1. INTRODUCTION

An ideal vascular graft should have desirable biocompatibility and suitable mechanical properties. Despite the successful application of man-made polymers (Dacron, PTFE, etc.) in large-diameter (≥6 mm) vascular grafts,[1] small-diameter (<6 mm) grafts are rarely used clinically, because of acute thrombogenicity, graft occlusion and other problems caused by inflammatory responses.[2]

In the blood circulatory system, thrombus formation involves the accumulation of circulating platelets at the injury site, as well as the coagulation system that produces thrombin and ultimately fibrin to stabilize the clot.[3] Although thrombosis plays a key role in preventing blood leakage in vessel injuries, it is also the major cause to the failures of small-diameter grafts.

Over the past decades, numerous efforts have been dedicated to developing blood vessels. Research findings showed that antithrombotic performance could be largely improved by combining surface modification, manufacturing methods and tissue culture systems together.[4−12] However, the most intensively studied strategies so far are heparin loading and endothelialization.[13−19] The former usually refers to the addition of heparin, a common anticoagulant used clinically, to the luminal surface of the graft, while the latter involves culturing of autologous endothelial cells in vitro to form a cell monolayer before transplantation.

Apart from thrombosis, biodegradation behavior was also found to be vital in vascular tissue engineering.[20−23] Because the mismatch between degradation speed and tissue regeneration would result in blood leakage and mechanical failure, the selection of degradable polymers is vital for tissue-engineered blood vessels.

In the present study, two commonly used antithrombotic methods, heparin loading and pre-endothelialization were used. Heparin was incoporated into the P(LLA-CL) nanofibers via coaxial electrospinning to form the heparin-loaded graft, whereas pre-endothelialized graft was prepared by seeding endothelial cells on the luminal surface of the pure P(LLA-CL) grafts with a self-developed dynamic endothelialization device. Mechanical properties of the grafts and the in vitro heparin release behavior were examined before surgery. All the grafts were implanted into canine femoral arteries for three months. Digital subtraction angiography (DSA), color Doppler flow

Received: January 9, 2013
Accepted: March 6, 2013
Published: March 6, 2013

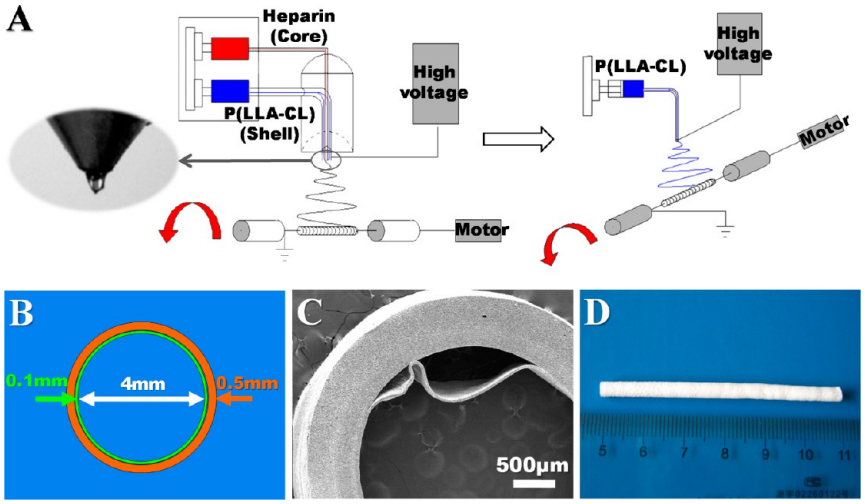

Figure 1. (A) Schematic diagram of the electrospinning process. (B–D) schematic, SEM, and digital camera images of the heparin-loaded tubular grafts.

imaging (CDFI), tensile testing, and hematoxylin and eosin (H&E) staining were performed to compare the physical and histological properties of the grafts after implantation.

2. MATERIALS AND METHODS

2.1. Materials. P(LLA-CL) (130 kDa) with 50% L-lactide (Gunze Limited, Japan) was dissolved in 2,2,2-Trifluoroethanol (TFE, Shanghai Fine Chemicals) at a concentration of 6%. The core solution was obtained by dissolving heparin (13 kDa, Runjie Medicine Chemical, China) in distilled water at the concentration of 12%. All reagents used for cell culture were purchased from Gibco Life Technologies, USA unless specified.

2.2. Fabrication. Heparin-loaded tubular grafts were fabricated using a purpose-made electrospinning setup and the process was depicted in Figure 1A. The inner layer was composed of fibers from coaxial electrospinning, in which the core solution (heparin) was injected at the flow rate of 0.1 mL/h and the shell solution (P(LLA-CL)) was injected at the rate of 0.8 mL/h. The outer layer was fabricated from P(LLA-CL) solution at the flow rate of 1.0 mL/h. A rotating mandrel with a diameter of 4 mm was used as the collector. The electrospinning time was 1 h for the inner layer and 4 h for the outer layer, the applied voltage was 18 kV and the collecting distance was limited to 15 cm. For comparison, scaffolds from pure P(LLA-CL) solution were also electrospun (electrospinning time = 5 h) as control.

During electrospinning, all fibers were obtained at an ambient temperature of 22–25 °C with a relative humidity of 40–50%. The scaffolds were desiccated in vacuum for 48 h prior to further characterization.

2.3. Physical Characterization. Fiber morphology was observed with a scanning electronic microscope (SEM, JSM-5600, Japan). The tubular scaffolds were immersed into liquid nitrogen and rapidly cut with a scalpel to generate a cross-section that the edge of the layers could be seen. Fiber diameter and layer thickness were estimated using image analysis software (Image-J, National Institutes of Health, USA).

Verification of the core–shell structure of the heparin-loaded fiber was conducted by TEM (H-800, Hitachi) at 100 kV. The sample was prepared by collecting the nanofibers onto carbon-coated Cu grids.

Mechanical measurement was performed using a universal materials tester (H5 K–S, Hounsfield, UK) with a 50 N load cell at ambient temperature. The grafts (n = 6) were cut open and a cross-head speed of 10 mm/min was used for all the specimens tested.

2.4. In vitro Release of Heparin. Heparin-loaded P(LLA-CL) grafts were suspended in PBS (pH 7.4) solution in sealed 6-well plates. The nanofibrous scaffolds were incubated under static conditions at 37 °C with the presence of 5% CO_2. At various time points, 1.0 mL supernatant was retrieved from the wells and an equal volume of fresh medium was replaced. The concentration of each retrieved heparin solution was then determined by toluidine blue method. Toluidine blue (3.0 mL) was added into the supernatant which was retrieved from the wells and reacted adequately with heparin for 2 h at 37 °C. Hexane (3.0 mL) was then added, and stirred vigorously to separate the heparin–toluidine blue complex formed. The aqueous solution of the samples was tested at 630 nm by an Agilent UV–vis spectrophotometer (WFH-203B, Perkin-Elmer, USA).

2.5. Dynamic Endothelialization. *2.5.1. Cell Harvest.* Endothelial cells (ECs) were isolated from dog autogenous femoral vein (about 3 cm length) by the method of enzyme digestion. After being washed by phosphate buffered saline (PBS) for 3 times, the femoral vein was applied in an in-site cannulation technique to avoid smooth muscle cell contamination and filled with 0.25% trypsin for 6 min in a cell incubator. Then the EC suspension was washed down by Dulbecco's modified Eagle's medium (DMEM) containing proper concentrations of VEGF and ECAF (Gibco, USA) from the vein and transferred into a 15 cm centrifuge tube. After centrifugation for 5 min, the cells were resuspended with culture medium in a culture flask and incubated at 37 °C in a humidified atmosphere containing 95% air and 5% CO_2. Replicated cultures were performed by trypsinizing the cells in PBS buffer when approaching confluence.

2.5.2. Dynamic Cell Culture. The proliferated cells were seeded into electrospun grafts from pure P(LLA-CL) by using a specially designed bioreactor (Figure 4A). Briefly, the tubular graft was embedded into a sterilized polypropylene tube (inner diamter = 5 mm) with one end sealed by a 220 nm filter. Before sealing the other end, the tube was filled with cell suspension at the density of 300 000/mL and then placed on a roller mixer at the rotation speed of 5 rpm. The whole system was put into a cell incubator to allow the dynamic cell culture. Cells were fed with medium every 24 h to avoid any insufficiency of gas exchange in the culture vessels.

2.5.3. Cell Morphology. After 7 days of culture, the tubular grafts were cut open and examined by SEM. The scaffolds were rinsed three times with PBS and fixed in 4% glutaraldehyde aqueous solution at 4 °C for 2 h. Fixed samples were rinsed with PBS and then dehydrated in graded concentrations of ethanol (30, 50, 70, 80, 90, 95, and 100%). After being dried in vacuum overnight, the cellular constructs were coated with gold sputter and observed under the SEM at a voltage of 10 KV.

For observing individual cells, the cultured scaffolds were cut open and washed with sterilized PBS for three times to remove medium and unviable cells, followed by immersing in a PBS solution containing 2% paraformaldehyde for 10 min at room temperature. After rinsing with PBS for three times, the scaffolds were placed in a permeabilization solution (0.2% Triton X-100 in PBS, Sigma-Aldrich) at room temperature for 10 min and rinsed again with fresh PBS for three

times. The scaffolds were then stained with 4, 6-diamidino-2-phenylindole (dilution ratio of 1:100, vol/vol) and phalloidin alexa 568 (dilution ratio of 1:100, vol/vol) overnight in dark environment. After rinsing with PBS for three times to remove the residual fluorescent dye, the matrices were ready for imaging under confocal microscope (Leica TCS SP5).

2.6. Implantation. In this study, all experimental procedures involving animals were conducted under Institutional Animal Care guidelines and approved ethically by the Administration Committee on Experimental Animals (Shanghai, China).

Eight Beagle dogs weighting 15−20 kg were anaesthetized by intravenous injection of sodium pentobarbital (30 mg/kg). The dogs were randomly separated into two groups(4 dogs for pre-endothelialized vascular grafts and the endothelial cells were isolated from the same dog as implanted, the other 4 dogs for heparin loaded grafts and all dogs chose the pure P(LLA-CL) scaffolds as the controls).

A bilateral femoral arteries implant model was applied in this study, as shown in Figure 5A. Segments of the femoral arteries (4 cm in length) were removed bilaterally while both sides of the arteries were clamped. The pretreated 5 cm length vascular grafts were then implanted into the femoral arteries using 7−0 Prolene sutures. The incision was sealed carefully with 4−0 silk sutures. All the dogs were given oral asprin at a dosage of 300 mg/day on the day of surgery and the next 7 days thereafter.

One week, two weeks, one month and three months after graft implantation, DSA and CDFI were performed repeatedly to visualize the patency of the implanted scaffolds. At the end of 3 months, the animals were killed humanely by overdosed pentobarbital and the implanted grafts were extracted for mechanical and histological analyses.

2.7. Mechanical and histological Characterizations of the Implanted Grafts. To conduct the tensile test, the implanted tubular grafts were cut into circular rings of 0.5 cm length ($n = 6$) and fixed in the Panlab organ bath system (ADInstruments, Spain). After fixation in the organ bath, the longitudinal tension was measured by force transducers (MLT0420, ADInstruments), recorded with a quad bridge amplifier (FE224, ADInstruments) connected to an analog-to-digital converter (ML870 Powerlab, ADInstruments) and analyzed by the Chart 5 software (ADInstruments). The maximal tension of tubular grafts was expressed as the total gram of tension per gram of the ring dry weight (g/g).

To observe the proximal, middle and distal cross-sectional end of the implanted grafts, the segments were cut and fixed with 4% paraformaldehyde, sliced into paraffin-embedded sections and H&E staining was performed by conventional procedures.

3. RESULTS

3.1. Morphology of the Grafts and Fibers. The heparin loaded graft, having an inner diameter of 4 mm and a length of 5 cm, were composed of two layers. The outer layer (0.5 mm in thickness) was formed by pure P(LLA-CL) nanofibers, while the inner layer (0.1 mm in thickness) was formed by heparin (core) and P(LLA-CL) (shell) nanofibers obtained from coaxial electrospinning. As shown in Figure 2, the average diameter of heparin-loaded P(LLA-CL) nanofibers and pure P(LLA-CL) nanofibers were 321 and 506 nm, respectively. According to the histogram, pure P(LLA-CL) fibers have a wider diameter distribution when compared to that of heparin-loaded P(LLA-CL) fibers. The cross-sectional view proved that the fibers were arranged evenly to allow a stable structure with pore size in the range from hundreds of nanometers to several micrometers.

3.2. Mechanical Properties of the Tubular Grafts. Representative tensile stress−strain curves of the electrospun nanofiber mats are shown in Figure 3A. The average strength of heparin-loaded P(LLA-CL) nanofiber mats were 5 MPa lower

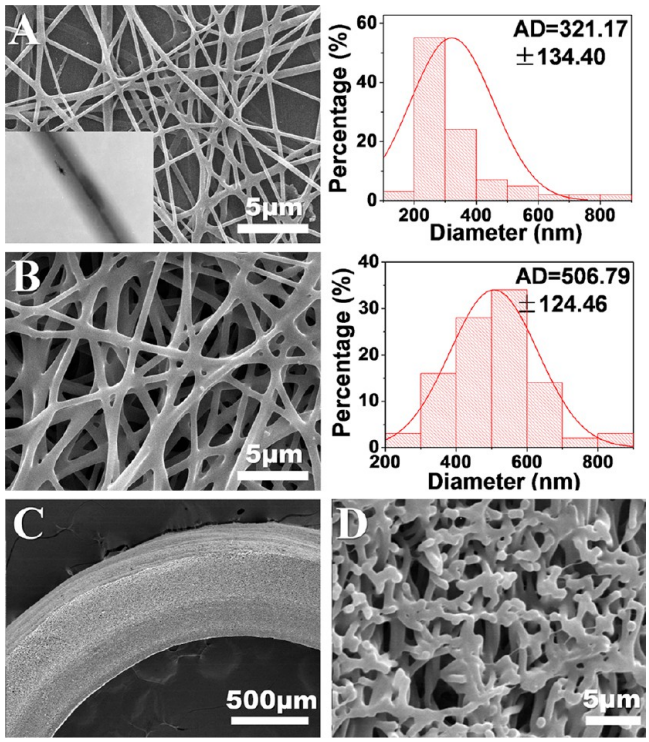

Figure 2. SEM images and the histogram of fiber diameter distribution. (A, B) Heparin-loaded P(LLA-CL) nanofibers (inset is the TEM iamge of a single nanofiber) and P(LLA-CL) nanofibers respectively; (C, D) SEM images of the cross-sectional view of a heparin-loaded graft at different magnifications.

than that of the pure P(LLA-CL) nanofiber mats. The encapsulation of heparin resulted in a lower ultimate strength and strain. However, the mechanical demand for vascular tissue engineering could still be met by the shell P(LLA-CL) part, as the average strength of heparin-loaded P(LLA-CL) nanofiber mats reached a maximum of 17.8 MPa with an elongation of 500%.

3.3. In vitro Release of the Heparin-Loaded P(LLA-CL) Nanofibers. To ensure that heparin was properly loaded, the in vitro release measurement was conducted for 14 days. The theoretical weight of heparin was 0.012 g, according to the concentration of solution and electrospinning time. In the aqueous solution, the release of heparin was found to experience two stages: the initial burst release at day 1 and the continuous release from day 2 to day 14. When exposed to PBS buffer, 20% of the heparin (0.012 g) was immediately released and the amount increased to 50% (0.0024 g) by the end of the first day. When the burst release was finished, a sustained release could be observed as the curve showed a stable ascending trend. The total amount of the released heparin was approximately 72% (0.0086 mg) after 14 days.

3.4. Dynamic Endothelialization. Pre-endothelialization was also used to achieve the antithrombotic property of the vascular graft. To achieve this goal, dynamic endothelialization was performed on the luminal surface of P(LLA-CL) tubular grafts. After 7 days of culture, the luminal surface was covered by a monolayer of well-spread endothelial cells, as shown in Figure 4B. The cell monolayer could be further demonstrated by the SEM image from Figure 4C. It should be noted here that a large number of cracks could be observed from the SEM, which were probably because that the dehydrated cell

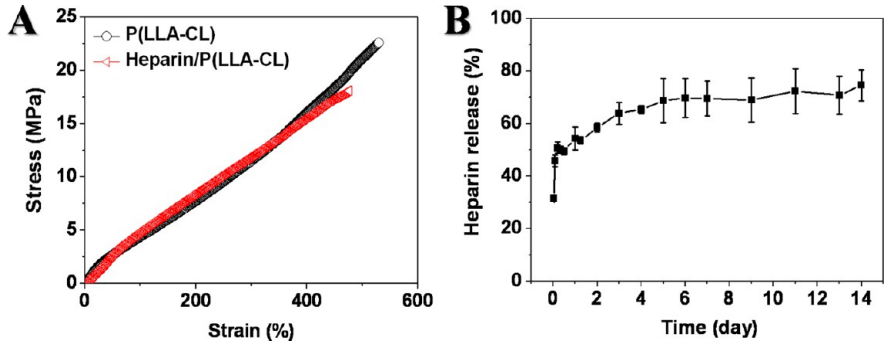

Figure 3. (A) Representative stress−strain curves of P(LLA-CL) and heparin-loaded P(LLA-CL) nanofiber grafts; (B) in vitro release of heparin from the heparin-loaded P(LLA-CL) nanofibers.

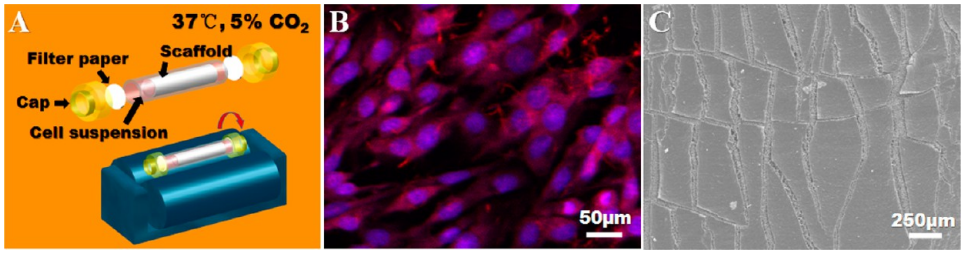

Figure 4. (A) Schematic diagram of the dynamic endothelialization device; (B, C) representative confocal microscope and SEM image of the endothelial cells after 7 days of culture.

monolayer was ruptured after the tubular-shaped graft was cut open and flattened to a two-dimensional, sheetlike membrane.

3.5. Patency Rate of the Implanted Grafts. Figure 5 shows the typical DSA and CDFI images of the blood inflow into the arteries (Video of the DSA could be found in the Supporting Information). Blood flow was blocked when passing through the P(LLA-CL) graft, but passed through the heparin loaded and pre-endothelialized grafts smoothly with clear blood flows being traced by CDFI. Based on the DSA results, patency rates at scheduled time points are summarized in Table 1. P(LLA-CL) grafts showed a poor patency rate from the very beginning, as only five of the eight arteries remained unblocked at week 1 and the number dropped to one 3 months later. In comparison, both heparin loaded graft and pre-endothelialized grafts had a 100% patency at week 2 and a 75% patency even after 3 months of implantation.

3.7. Tensile Properties. Table 1 clearly shows that the average tension and elongation of the implanted grafts are slightly weaker than those of autologous grafts. With the incorporation of heparin, the tension of the P(LLA-CL) grafts decreased from 97868 g/g dry weight to 83689 g/g, whereas the elongation exhibited an increase from 7.2 mm to 7.7 mm. The pre-endothelialized grafts had an average tension of 95776 g/g and elongation of 8.8 mm, indicating a better flexibility in comparison with the other two types of electrospun grafts.

3.8. Histological Analyses. Figure 6 indicates the H&E staining images of the implanted grafts. For the heparin-loaded grafts, a clear monolayer of endothelial cells was observed at the proximal end, as shown in Figure 6A. However, no monolayer could be found at the middle or distal ends. For the pre-endothelialized grafts, the cells showed a sound growth and the entire luminal surface was covered by a cell monolayer. Moreover, some cells seemed to infiltrate into the electrospun grafts, as illustrated by the arrows in Figure 6D−F. The graft made of pure P(LLA-CL), on the other hand, exhibiting no

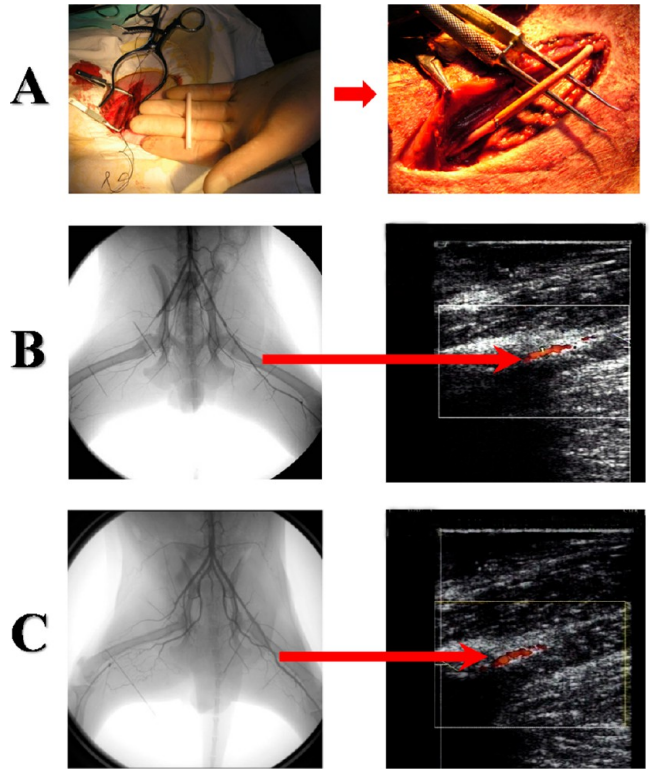

Figure 5. (A) Surgical implantation of the electrospun tubular graft into the femoral artery of Beagle dog. Typical DSA and CDFI inspection of (B) heparin-loaded and (C) pre-endothelialized grafts after 3 months: the left femoral artery was replaced by heparin-loaded or pre-endothelialized graft, and the right one was replaced by P(LLA-CL) graft. Blood flow in the left femoral artery was further traced by the CDFI image.

dx.doi.org/10.1021/am400099p | ACS Appl. Mater. Interfaces 2013, 5, 2220−2226

Table 1. Patency Rate and Tensile Results of the Tubular Grafts

	patency rate					
sample	week1	week 2	month 1	month 3	tension (g/g)	elongation (mm)
P(LLA-CL)	5/8	4/8	2/8	1/8	97868 ± 264	7.2 ± 1.1
Heparin/P(LLA-CL)	4/4	4/4	3/4	3/4	83689 ± 278	7.7 ± 1.4
pre-endothelialization	4/4	4/4	3/4	3/4	95776 ± 193	8.8 ± 1.7
autologous					108400 ± 547	10.9 ± 1.7

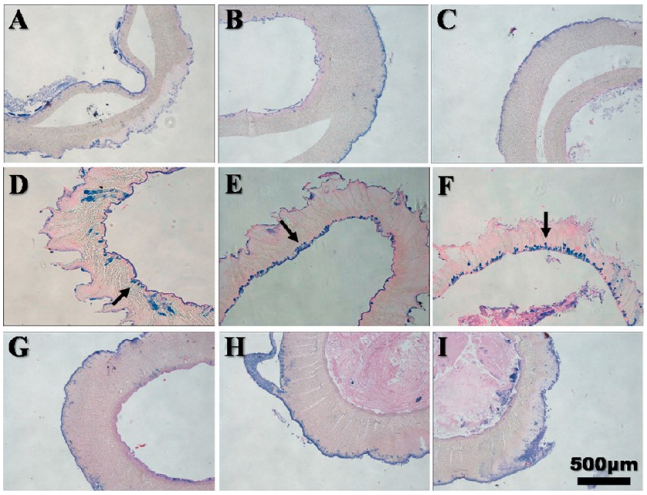

Figure 6. H&E staining of the implanted grafts after 3 months. (A–C) Proximal, middle, and distal cross-sectional images of the heparin loaded graft, respectively; (D–F) proximal, middle, and distal cross-sectional images of the pre-endothelialized graft, respectively; and (G–I) proximal, middle, and distal cross-sectional images of the P(LLA-CL) graft respectively, thrombi were shown in both H and I. The black arrows point out the cell monolayers formed on the luminal surface.

endothelial cell growth and the lumen was blocked by blood clots.

4. DISCUSSION

Electrospinning was used to produce the fibrous grafts because it is a versatile and intensively studied method to get nanofibers, which structurally mimic the native extracellular matrices (ECMs).[24] The versatility of electrospinning allows numerous natural and synthetic materials to be electrospun into tubular-shaped scaffolds for vascular tissue engineering.[25−27] However, only a few products have entered into the medical market so far, mainly due to the low patency rate and the unstable performances of vascular scaffolds in vivo. The aim of this study was to make a preliminary in vivo comparison between the two mostly investigated antithrombosis approaches, heparin loading and pre-endothelialization.

To examine the influencing factors of patency rate by a comparatively simple model, we used P(LLA-CL) and heparin as the starting material. Our previous work has found that P(LLA-CL), a synthetic copolymer of L-lactide and Caprolactone, had good mechanical properties as well as good biocompatibility. Both smooth muscle cells and endothelial cells proliferated well on the P(LLA-CL) nanofibers.[28,29] What's more, the strength, elasticity and biodegradation rate of P(LLA-CL) can be adjusted by changing the molar ratios of PLLA in the copolymer.

Physical characterizations of the grafts were determined before implantation. Electrospun scaffolds usually have a high porosity but a densely packed structure. While such structure hampers the inside growth of cells, it is conducive to prevent blood from penetrating into engineered vascular grafts. Nanofibers electrospun from P(LLA-CL) had a larger average diameter than that of heparin-loaded fibers, which was attributed to the difference in the flow rate of P(LLA-CL) solution. When using the same electrospinning solution and setting electrostatic force as constant (18 kV), fibers were believed to undertake more stretch and attenuation under a lower flow rate.[30] The core–shell jet from the spinning nozzle (Figure 1A) illustrated that by coaxial electrospinning, heparin was finely incorporated in the core part of P(LLA-CL) nanofibers. Such a core–shell structure could be further demonstrated by the inset TEM image in Figure 2A. For heparin-loaded grafts, the shell part of P(LLA-CL) nanofiber prevented the scaffold from a dramatically mechanical loss, as demonstrated by the stress–strain curves in Figure 3A. The mechanical similarity of core–shell and pure P(LLA-CL) nanofibers also played an indispensable role, as the core–shell fibers would not be easily broken into segments under pressure. Another advantage of such a structure is that it can secure a controlled release of heparin for a peroid as long as 14 days. Thus, a larger amount of heparin could be sealed when immersing the scaffolds into aqueous solution.

For the pre-endothelialized grafts, whether cells could cover the scaffolds may directly affect the deposition of platelets and the formation of thrombus. Therefore, both confocal microscopy and SEM were used to observe how long the monolayer of endothelial cells could be formed. The results in Figure 4 showed that under the seeding density of 300 000/mL, the cells spred and proliferated well on the luminal surface of the grafts after 7 days of culture. For this reason, all the pre-endothelialized grafts were cultured in vitro for 7 days before implantation.

In this study, we chose Beagle dogs to set up vascular graft implantation model, as the size, structure and mechanical properties of the femoral arteries in dogs were highly similar to those of human beings, which makes dogs an ideal model for long-term in vivo study.[31] Moreover, by using large animals like dogs, two grafts can be implanted in the femoral arteries of one animal, allowing us to make a direct comparison of the patency rates.

Small-sized synthetic tubular grafts could be easily blocked if no further treatment was applied.[32] As expected, the P(LLA-CL) group showed a poor patency rate (67.5%) from the beginning and the condition got worse (12.5%) after 3 months. The four heparin-loaded grafts, on the other hand, all remained patent for more than 2 weeks. Only one of the grafts was blocked after 1 month, and the total patency rate was 75% after 3 months of implantation, indicating an obvious improvement in patency rate. The situation was similar in the pre-endothelialized group, whose patency rate was also 75% after 3 months. Although the results here were based on a comparatively small number of samples, it still strongly suggested the improvement of patency rate. Figure 5 shows a

more visualized comparison: blood flow was unable to pass through the right artery (P(LLA-CL) graft) but was going smoothly at the left one (heparin-loaded graft).

Although no difference in patency rates was found between heparin loading and pre-endothelialization, it is noticeable that the tensile properties of endothelialized grafts were better than those of heparin-loaded grafts after three months of implantation. Both tension and elongtation were increased by 14% according to the data from Table 1, which is probably due to the difference in fiber structure (core−shell P(LLA-CL) fibers versus homogeneous P (LLA-CL) fibers). It should be noted that the formation of endothelial cell layer might also be positive to the mechanical improvement.[33,34] The tensile results also indicated that P(LLA-CL), the supporting material, could provide adequate strength and flexibility in vivo for at least 3 months. This is of particular importance in vascular tissue engineering, as scaffolds should not degrade too fast in vivo, so that the function of serving as cell carriers and providing structural support could be achieved.

Besides the difference in tensile results, the growth of endothelial cells also varied in different scaffolds. For the heparin-loaded grafts, a cell monolayer was formed at proximal end, but only few cells could be found at middle or distal end. The possible explanation is that at the proximal potion, neighboring autologous cells might migrate along with blood flow and proliferate to form a cell monolayer on the surface of the implanted scaffold. At the middle part, however, no cell monolayer could be found and the cell density was much lower even after three months of in vivo culture, suggesting that the migration speed of neighboring cells is very slow. On the contrary, no endothelial cells could be found at the distal end, probably because that the cells nearby were not able to move against the blood flow or the surface of the biosynthetic scaffolds was not amiable to anchor endothelial cells.

For the pre-endothelialized grafts, clear cell monolayers were observed anywhere regardless of the direction of blood flow. Such phenomenon demonstrated the in vivo survival of the preseeded cells. More interestingly, after three months of implantation, some of the cells infiltrated into the pores of the nanofibrous scaffolds, as illustrated by the arrows in Figure 6. One of the major problems in electrospun tissue engineered scaffolds is their tightly packed fibrous structure and small pore size, which impede the infiltration of cells. Although the grafts in our study were also highly packed with the pore size distribution in the range from hundreds of nanometers to several micrometers, we found that when the entire luminal surface was covered by endothelial cells, some of the cells were capable to infiltrate into the scaffolds. This finding is similar to our previous study and is believed to be beneficial to the three-dimensional repair of damaged tissue.[35] In vascular tissue engineering, another advantage of such a packed structure is the ability to prevent blood leakage, which ensured the success of implantation and future recovery.

As for the control group, no cell growth was found on the surface of the P(LLA-CL) grafts, even though the grafts were implanted into the same animal and experienced the same period of recovery. We speculate that most of the P(LLA-CL) grafts are blocked by blood clots at an early stage, thus hampering the migration of autologous endothelial cells.

Although both heparin loading and pre-endothelialization could greatly enhance the patency rate of small diameter P(LLA-CL) grafts in this study, such an improvement in patency rate might not be enough to meet the criteria in clinical settings, particularly when the vascular implantation period is mostly longer than 3 months. Thus, more efforts (ie, combination of heparin loading and pre-endothelialization, surface modification or blending with natural materials or proteins) are needed to further enhance the patency rate before a clinical trial is finally carried out.

CONCLUSION

In a canine femoral artery grafting model, we demonstrated that both heparin loading and endothelialization could significantly enhance the in vivo patency rates of small-diameter grafts. Heparin loading was a comparatively easy and economical way, whereas the pre-endothelialized strategy possessed better mechanical properties and cellular compatibility, which could be helpful for future design and development of electrospun vascular grafts. In addition, we also found that electrospun tubular grafts possessed suitable mechanical strengths both in vitro and in vivo when P(LLA-CL) was chosen as the basic material.

ASSOCIATED CONTENT

Supporting Information

Video of the DSA and bioactivity of heparin loaded in electrospun fibers. This material is available free of charge via the Internet at http://pubs.acs.org/.

AUTHOR INFORMATION

Corresponding Author

*E-mail: xmm@dhu.edu.cn (X.M.); oriental_wang@hotmail.com (S.W.).

Author Contributions

†C.H. and S.W. contributed equally to this paper.

Notes

The authors declare no competing financial interest.

ACKNOWLEDGMENTS

This study was supported by the Science and Technology Commission of Shanghai Municipality Program (11 nm0506200), National Nature Science Foundation of China (31070871, 31271035), the National Plan for Science and Technology (10-NAN1013-02) and the Reserved Academic Leader Program of Shanghai Tenth People's Hospital. The authors thank Prof. Tong Lin from Deakin University for his precious advice on the work.

REFERENCES

(1) Kannan, R. Y.; Salacinski, H. J.; Butler, P. E.; Hamilton, G.; Seifalian, A. M. *J. Biomed. Mater. Res., Part B* **2005**, *74*, 570−581.
(2) Isenberg, B. C.; Williams, C.; Tranquillo, R. T. *Circ. Res.* **2006**, *98*, 25−35.
(3) Li, S.; Henry, J. J. D. *Annu. Rev. Biomed. Eng.* **2011**, *13*, 451−475.
(4) L'Heureux, N.; Dusserre, N.; Konig, G.; Victor, B.; Keire, P.; Wight, T. N.; Chronos, N. A. F.; Kyles, A. E.; Gregory, C. R.; Hoyt, G.; Robbins, R. C.; McAllister, T. N. *Nat. Med.* **2006**, *12*, 361−365.
(5) L'Heureux, N.; McAllister, T. N.; de la Fuente, L. M. *New Engl. J. Med.* **2007**, *357*, 1451−1453.
(6) Hoenig, M. R.; Campbell, G. R.; Rolfe, B. E.; Campbell, J. H. *Arterioscler., Thromb., Vasc. Biol.* **2005**, *25*, 1128−1134.
(7) Zhang, J.; Qi, H.; Wang, H.; Hu, P.; Ou, L.; Guo, S.; Li, J.; Che, Y.; Yu, Y.; Kong, D. *Artif. Organs* **2006**, *30*, 898−905.
(8) Hong, Y.; Ye, S.-H.; Nieponice, A.; Soletti, L.; Vorp, D. A.; Wagner, W. R. *Biomaterials* **2009**, *30*, 2457−2467.

(9) Zheng, W.; Wang, Z.; Song, L.; Zhao, Q.; Zhang, J.; Li, D.; Wang, S.; Han, J.; Zheng, X.-L.; Yang, Z.; Kong, D. *Biomaterials* **2012**, *33*, 2880−2891.
(10) Du, F.; Wang, H.; Zhao, W.; Li, D.; Kong, D.; Yang, J.; Zhang, Y. *Biomaterials* **2012**, *33*, 762−770.
(11) Huang, C.; Chen, R.; Ke, Q.; Morsi, Y.; Zhang, K.; Mo, X. *Colloids Surf., B* **2011**, *82*, 307−315.
(12) Zander, N. E.; Orlicki, J. A.; Rawlett, A. M.; Beebe, T. P. *ACS Appl. Mater. Interfaces* **2012**, *4*, 2074−2081.
(13) Gutowska, A.; Bae, Y. H.; Feijen, J.; Kim, S. W. *J. Controlled Release* **1992**, *22*, 95−104.
(14) Li, Y.; Neoh, K. G.; Kang, E. T. *J. Biomed. Mater. Res., Part A* **2005**, *73A*, 171−181.
(15) Meinhart, J. G.; Deutsch, M.; Fischlein, T.; Howanietz, N.; Froschl, A.; Zilla, P. *Ann. Thorac. Surg.* **2001**, *71*, S327−331.
(16) Anderson, J. S.; Price, T. M.; Hanson, S. R.; Harker, L. A. *Surgery* **1987**, *101*, 577−86.
(17) Shirota, T.; Yasui, H.; Shimokawa, H.; Matsuda, T. *Biomaterials* **2003**, *24*, 2295−2302.
(18) Ye, L.; Wu, X.; Duan, H.-Y.; Geng, X.; Chen, B.; Gu, Y.-Q.; Zhang, A.-Y.; Zhang, J.; Feng, Z.-G. *J. Biomed. Mater. Res., Part A* **2012**, *100A*, 3251−3258.
(19) Ye, L.; Wu, X.; Mu, Q.; Chen, B.; Duan, Y.; Geng, X.; Gu, Y.; Zhang, A.; Zhang, J.; Feng, Z.-g. *J. Biomater. Sci., Polym. Ed.* **2011**, *22*, 389−406.
(20) Murugan, R.; Ramakrishna, S. *Tissue Eng.* **2006**, *12*, 435−447.
(21) Vijayan, V.; Shukla, N.; Johnson, J. L.; Gadsdon, P.; Angelini, G. D.; Smith, F. C. T.; Baird, R.; Jeremy, J. Y. *J. Vasc. Surg.* **2004**, *40*, 1011−1019.
(22) de Valence, S.; Tille, J.-C.; Mugnai, D.; Mrowczynski, W.; Gurny, R.; Möller, M.; Walpoth, B. H. *Biomaterials* **2012**, *33*, 38−47.
(23) Pandis, L.; Zavan, B.; Bassetto, F.; Ferroni, L.; Iacobellis, L.; Abatangelo, G.; Lepidi, S.; Cortivo, R.; Vindigni, V. *Microsurgery* **2011**, *31*, 138−145.
(24) Stevens, M. M.; George, J. H. *Science* **2005**, *310*, 1135−1138.
(25) Xu, C.; Inai, R.; Kotaki, M.; Ramakrishna, S. *Tissue Eng.* **2004**, *10*, 1160−1168.
(26) Amoroso, N. J.; D'Amore, A.; Hong, Y.; Wagner, W. R.; Sacks, M. S. *Adv. Mater.* **2011**, *23*, 106−111.
(27) Agarwal, S.; Wendorff, J. H.; Greiner, A. *Polymer* **2008**, *49*, 5603−5621.
(28) Mo, X. M.; Xu, C. Y.; Kotaki, M.; Ramakrishna, S. *Biomaterials* **2004**, *25*, 1883−1890.
(29) Zhang, K.; Wang, H.; Huang, C.; Su, Y.; Mo, X.; Ikada, Y. *J. Biomed. Mater. Res., Part A* **2010**, *93A*, 984−993.
(30) Deitzel, J. M.; Kleinmeyer, J.; Harris, D.; Beck Tan, N. C. *Polymer* **2001**, *42*, 261−272.
(31) Rashid, S. T.; Salacinski, H. J.; Hamilton, G.; Seifalian, A. M. *Biomaterials* **2004**, *25*, 1627−1637.
(32) Pektok, E.; Nottelet, B.; Tille, J.-C.; Gurny, R.; Kalangos, A.; Moeller, M.; Walpoth, B. H. *Circulation* **2008**, *118*, 2563−2570.
(33) Zorlutuna, P.; Rong, Z.; Vadgama, P.; Hasirci, V. *Acta Biomater.* **2009**, *5*, 2451−2459.
(34) Sirois, E.; Charara, J.; Ruel, J.; Dussault, J. C.; Gagnon, P.; Doillon, C. J. *Biomaterials* **1998**, *19*, 1925−1934.
(35) Chen, Z. G.; Wang, P. W.; Wei, B.; Mo, X. M.; Cui, F. Z. *Acta Biomater.* **2010**, *6*, 372−382.